

## Microbubble detection and separation by using patterned ultrasound plane wave

Junseok An<sup>1†</sup>, Naohiro Sugita<sup>2</sup>, and Tadahiko Shinshi<sup>2</sup> (<sup>1</sup>Dpt. Mech. Eng, Tokyo Tech; <sup>2</sup>FIRST, Tokyo Tech)

### 1. Introduction

Angiogenesis is a vital physiological process where new microvessels are formed within the existing vascular structure. Angiogenesis is crucial in predicting cancer progression and evaluating of bodily injuries<sup>1</sup>. However, conventional ultrasound imaging is limited in spatial resolution due to the diffraction limit determined by the sound wavelength, making it impossible to visualize microvascular structures. Super-resolution ultrasound imaging (SRU) surpasses the inherent diffraction limit through sub-diffraction techniques, enabling the visualization of microvascular structures.

SRU employs contrast agents known as microbubbles (MBs) to detect scattered signals and localize the point spread function (PSF) of MBs, enabling the determination of the MB positions<sup>2</sup>. Nevertheless, the acquisition time of conventional SRU is prolonged due to concentration limitations and the low detectability of MBs. The low detectability arises from attenuation of scattering waves owing to bubble-bubble mutual interaction. In high-concentration MBs, each bubble cannot be detected individually because the PSFs of each bubble overlap and become a single entity at that high concentration.

In this research, our primary objective is to reduce the acquisition time in SRU imaging. We propose an innovative ultrasound imaging method using patterned plane waves (PPWs) where phases of the sound waves are spatially patterned. We demonstrate that the PPWs improve the detectability of MBs by modifying bubble-bubble interactions, altering the acoustic intensity of MBs in an ultrasound image. Furthermore, we address concentration limitations, by leveraging the acoustic pressure distribution of PPWs. This enables to alter the PSF of each MB, which makes it possible to separate MBs with closer inter-distances than the sound wavelength.

### 2. Materials and Methods

#### 2.1 Dynamic model of MBs

Microbubbles repeatedly contract and expand in response to changes in the surrounding pressure, generating scattered ultrasound waves. The Rayleigh-Plesset equation coupled with Church's

shell model<sup>3</sup>) describes the radial variation of an elastic spherical bubble. In addition, by adding the coupling term between bubbles due to acoustic radiation, we can obtain the motion equation composed of  $x_n = R_n/R_{n0} - 1$  where  $R_n$  and  $R_{n0}$  are the temporal and equilibrium bubble radius, respectively. The coupled equation of motion describing the radial dynamics of spherical bubbles can be formulated as a set of the delayed ordinary differential equations as

$$\begin{aligned} & \ddot{x}_n(t) + \omega_{n0}\delta_n\dot{x}_n(t) + \omega_{n0}^2x_n(t) \\ &= - \sum_{\substack{m=1 \\ m \neq n}}^N \frac{R_{m0}^2}{R_{n0}d_{nm}} \ddot{x}_m\left(t - \frac{d_{nm}}{c}\right) + p_{an}(t) \end{aligned} \quad (1)$$

where  $x_n$  is the dimensionless displacement, and  $\omega_{n0}$ ,  $\delta_n$ ,  $d_{nm}$ , and  $c$  represent the natural angular frequency, the damping ratio, the separation distance between the m-th and n-th bubbles, and the speed of sound in the surrounding fluid, respectively. The first term on the right-hand side of Eq. (1) corresponds to the acoustic radiation pressure, where  $p_{an}(t)$  stands for the incident acoustic pressure measured at the center position of n-th bubble.

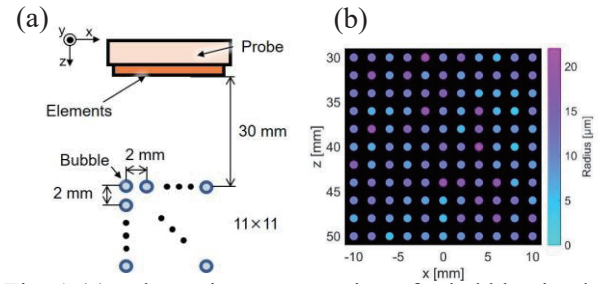


Fig. 1 (a) Schematic representation of a bubble cloud containing 121 MBs. (b) The size distribution of the bubble cloud.

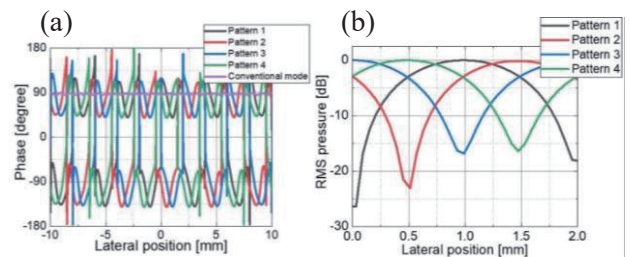


Fig. 2 Comparison of phases of the conventional ultrasound beam and the proposed PPWs. (b) RMS pressure distribution of PPWs.

E-mail: <sup>†</sup>an.j.ad@m.titech.ac.jp, \*sugita.n.aa@m.titech.ac.jp

## 2.2 Beam patterning

**Fig. 1(a)** represents a schematic illustration of the simulation model with 121 MBs arranged in an  $11 \times 11$  grid pattern. The ultrasound probe used is a linear array with 64 elements of 0.5 mm in width, and the center frequency of 1.4 MHz. **Fig. 1(b)** describes the size distribution of the bubble cloud. The mean radius is 11  $\mu\text{m}$  and the standard deviation is 4  $\mu\text{m}$ .

A PPW is formed by grouping every four elements and alternating in-phase and anti-phase burst voltage signals into the groups. **Fig. 2(a)** shows the pressure phase of PPWs at the central frequency. By shifting the 4-element-groups by one element, we can utilize four beams with different spatial patterns (Pattern 1 to 4). The conventional mode is a plane wave and compared with the PPWs for reference. The root-mean-square pressure of the incident wave measured at  $z=30$  mm is presented in **Fig. 2(b)**. We receive scattered waves at each element and perform acoustic imaging of the bubble cloud. Acoustic imaging simulations were conducted using MATLAB.

## 3. Results

Initially, we investigated a single isolated bubble exposed to the conventional plane wave. The bubble radii are standardized at 10  $\mu\text{m}$ . The resulting acoustic image is presented in **Fig. 3(a)**. Bubble detection was performed by identifying the intensity peak within the acoustic image. The highest intensity observed in **Fig. 3(a)** was used as the reference threshold for detecting bubbles throughout this study.

To validate the capability of PPWs in bubble detection, we examine the overall number of detected bubbles using both conventional and proposed methods. In **Fig. 3(b)**, the quantity of identified bubbles is shown for the case of the bubble cloud. Due to the ability of PPWs to detect bubbles that remain undetectable by plane waves, the cumulative detection count surpasses that of the conventional method. We introduce a new detection rate, calculated as the ratio between total detections utilizing PPWs and those using only the conventional method. This follows that by sequentially employing PPWs within a short time, the total count of detectable bubbles can be enhanced, potentially reducing in imaging time.

The effectiveness of PPWs in prompting bubble separation is confirmed through a numerical experiment involving three bubbles. **Fig. 4(a)** represents a normalized acoustic image acquired using the conventional method, where the three bubbles are positioned so closely together that their PSFs overlap and appear as a single entity due to the spatial resolution limit. **Fig. 4(b)** illustrates the subtracted image achieved by subtracting the image

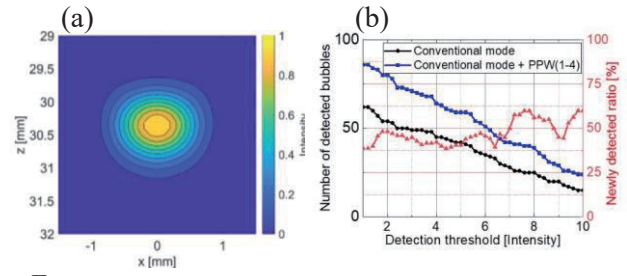


**Fig. 3** (a) Simulated acoustic image for single bubble when using the conventional mode. (b) Number of newly detected bubbles by PPWs.

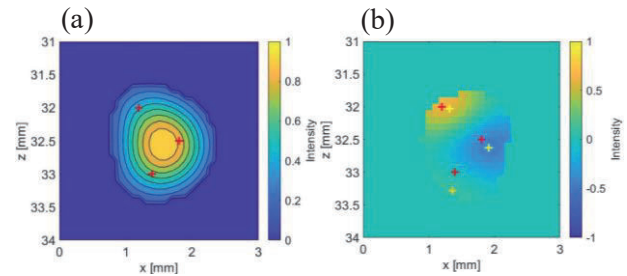


**Fig. 4** (a) Simulated normalized acoustic image of 3 bubbles using the conventional mode. (b) Pixeled image obtained by subtracting Pattern 1 from Pattern 3.

obtained using Pattern 1 from the image using Pattern 3. The red cross markers correspond to the actual bubble positions, while the yellow markers represent the centers of full width half maximum regions of the subtracted PSFs. It was demonstrated that it is feasible to determine the positions of bubbles located closely by utilizing PPWs.

## 4. Conclusion

We conducted acoustic imaging simulations that account for bubble-bubble interaction, thus verifying the efficacy of PPWs in detecting and separating MBs. Using PPWs amplifies the capability to detect MBs and enables the differentiation of MBs positioned closer than the inherent spatial resolution. This ability surpasses the constraints of bubble concentration limitation. Therefore, PPWs demonstrate the potential to minimize the acquisition time of SRU imaging.

## Acknowledgment

This work was supported by JSPS KAKEN Grant Number 23K13276.

## References

- 1) P. Carmeliet and R. K. Jain, *Nature*, **407**, 6801 (2000).
- 2) K. Christensen-Jeffries et al., *Ultrasound in Med. & Biol.*, **46**, 4 (2020).
- 3) C. C. Church, *J. Acoust. Soc. Am.*, **1**, 97 (1995).